

ABSORB: Atlas Building by Self-Organized Registration and Bundling

Hongjun Jia¹, Guorong Wu¹, Qian Wang^{1,2} and Dinggang Shen¹

¹Department of Radiology and BRIC, ²Department of Computer Science
University of North Carolina at Chapel Hill, Chapel Hill, North Carolina, 27599, USA
{jiahj, grwu, dgshen}@med.unc.edu qianwang@cs.unc.edu

Abstract

A novel groupwise registration framework, called *Atlas Building by Self-Organized Registration and Bundling (ABSORB)*, is proposed in this paper. In this framework, the global structure of relative subject image distribution is preserved during the registration by constraining each subject to deform locally within the learned manifold. A self-organized registration is employed to deform each subject towards a subset of its neighbors that are closer to the global center. Some subjects close enough in the manifold will be bundled into a subgroup during the registration, and then deformed together in the subsequent registration process. This framework performs groupwise registration in a hierarchical way. Specifically, in the higher level, it will perform on a much smaller dataset formed by the representative subjects of all subgroups generated in the previous levels of registration. The atlas image can be eventually built once the registration arrives at the upmost level. Experimental results on both synthetic and real datasets show that the proposed framework can achieve substantial improvements, compared to the other two widely used groupwise methods, in terms of both registration accuracy and robustness.

1. Introduction

Image registration is one of the most important techniques in the field of medical image analysis due to its significance in both scientific researches and clinical applications [1-3]. To better understand and analyze the group similarity and variation within a population, many groupwise registration methods have been proposed to achieve more accurate and consistent registration by registering all images simultaneously [4-11].

Several groupwise registration methods are proposed to directly register all images by formulating the groupwise registration as an optimization problem with a global cost function. In the congealing registration method [5] and its extensions [6,12], an objective function is defined over all aligned images in the dataset, to solve the groupwise registration by a gradient-based optimizer. However, the

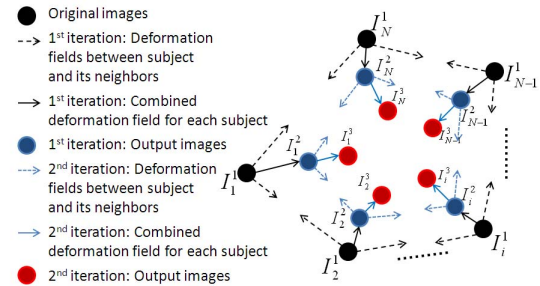


Figure 1: The framework for the proposed ABSORB algorithm. huge number of variables involved in the global cost function poses challenges to the optimizer which is vulnerable to local minima. Joshi *et al.* [7] proposed to solve the groupwise registration in an iterative manner by registering each subject to the mean image and updating the mean based on the newly registered images. This method can provide an unbiased way to build the atlas, and also can converge fast. However, the registration of this method could be misled by trying to register sharp individual images (with clear anatomical structures) to a blurry group mean image (without clear anatomical details), especially in the first rounds of registration.

It is generally difficult to achieve good registration in one step by simply registering each image to an explicit (or implicit) template directly, especially when anatomical variations are large across images within the group. To this end, a few algorithms have been proposed to register the individual image to the template with the help of intermediate templates [13-16]. For example, in [13], after learning the intrinsic manifold on the dataset, the pseudo-geodesic median is determined as the template, and the corresponding geodesic paths between each image and the template are computed to form a tree on the learned manifold. Since a fixed image is used as the final template to register all other images, the deviation from the group center is unavoidable if the template cannot represent the dataset, although the registration error could be reduced since only the nearby images need to be registered.

A new framework for groupwise registration, termed as *Atlas Building by Self-Organized Registration and Bundling*, or ABSORB for short, is proposed in this paper to address the problems mentioned above, as illustrated in Fig.1. We resolve the groupwise registration in an iterative

way by warping each image to the common space step by step on the learned manifold, and maintain the relative global distribution of the population at the same time. To achieve this goal, two new strategies, namely self-organized registration and image bundling, are proposed. Specifically, the self-organized registration is introduced to deform each image towards a subset of its neighbors that are closer to the global center and thus condense the distribution of images on the learned manifold gradually. Some nearby subjects get close enough to each other during the registration and are bundled into a subgroup. ABSORB can thus perform the groupwise registration hierarchically. Particularly, in the higher level, the registration is performed on a much smaller dataset, which consists of the representative images of all subgroups formed in the previous registration steps. As the result of this hierarchical registration process, a pyramid of images is built automatically and the atlas image can be generated once the registration arrives at the upmost level.

2. Method

The new groupwise registration framework, *i.e.* ABSORB, is presented in this section. We assume that $\mathbf{I} = \{I_1, I_2, \dots, I_N\}$ with N images has already been pre-processed after affine registration. The registered image of subject I_i at the beginning of iteration t is denoted as I_i^t , where $i = 1, 2, \dots, N$ and $t \geq 1$. The goal of ABSORB at iteration t is to further align all images $\mathbf{I}^t = \{I_1^t, I_2^t, \dots, I_N^t\}$ and obtain an updated set $\mathbf{I}^{t+1} = \{I_1^{t+1}, I_2^{t+1}, \dots, I_N^{t+1}\}$, so that all the images in \mathbf{I}^{t+1} are distributed more densely in the data space. Here, we set $\mathbf{I}^1 = \mathbf{I}$.

The registration process of the proposed framework is illustrated in Fig. 1. To deform I_i^t towards the common space at the t^{th} iteration, a self-organized registration is first performed. Specifically, some qualified neighbors of I_i^t are selected, and then the deformation field defined to warp I_i^t to I_i^{t+1} is calculated based on the deformation fields between I_i^t and its selected neighbors. In this paper we use the diffeomorphic demons in ITK [3] to implement the pairwise registration. After performing the self-organized registration on all subjects in iteration t , we bundle some nearby subjects into respective subgroup if they have been aligned well to each other, and then update the deformed image set \mathbf{I}^t with \mathbf{I}^{t+1} . The same procedures are repeated on \mathbf{I}^{t+1} until the algorithm converges.

2.1. Selection of neighboring subjects

The selection of neighboring subjects is critical to self-organized registration. A particular procedure is designed to adaptively choose a subset of neighbors for each subject by considering both local and global information. To achieve it, a graph is built with each subject I_i^t as a node and each edge connecting I_i^t and I_j^t weighted by the

distance between them. The distance could be the intensity difference or that defined in [13]. To better measure the distance between two subjects on the data space, a k -NN isomap is constructed following the procedure in [17]. So the distance between I_i^t and I_j^t can be defined as $d(I_i^t, I_j^t) = d_m(I_i^t, I_j^t)$, where $d_m(I_i^t, I_j^t)$ is the shortest distance between I_i^t and I_j^t on the learned manifold.

In order to reach the final atlas (or the global center) in an efficient way, we embed the global center information into the selection of neighboring subjects. When selecting the qualified neighbors of one subject for registration, only those subjects that are closer to the global center than the subject under consideration are selected. Here, the global center is different from a fixed template in two ways: 1) the global center is not served as a template; 2) the global center is updated online (rather than being fixed as in most other registration methods), and it is only used to provide general information to the selection of qualified neighbors.

The determination of global center is important to the performance of the algorithm as it guides the registration in each iteration. We select the median image on the learned manifold as the global center due to its robustness to the outliers as shown in [13]. The median subject in a dataset is defined as the subject that minimizes the overall distance from that subject to all other subjects. Instead of building a fixed graph throughout the registration process, we propose a dynamic graph which is updated on the dataset composed of the registered images after each round. The global center is then updated accordingly on the manifold. This helps subjects adjust the moving directions more adaptively. However, if the graphs in different iterations are built independently, the determined global center may change dramatically, and thus the estimated deformation for each subject would lack continuity in the perspective of registration process. To obtain a consistent but not fixed global center, we build an Iterative Neighborhood Graph (ING), \mathcal{G}^t , from the k -NN isomap. The weight assigned to the edge connecting two images I_i^t and I_j^t in \mathcal{G}^t is defined as

$$w(I_i^t, I_j^t) = \begin{cases} d(I_i^t, I_j^t) + \alpha \cdot w(I_i^{t-1}, I_j^{t-1}), & t > 1, \\ d(I_i^1, I_j^1) & , t = 1, \end{cases} \quad (1)$$

where the current edge weight $w(I_i^t, I_j^t)$ is calculated as a weighted summation of $d(I_i^t, I_j^t)$ and $w(I_i^{t-1}, I_j^{t-1})$. The median image $I_{c(t)}^t$ (or the global center) is selected by

$$c(t) = \arg \min_i \sum_j w(I_i^t, I_j^t). \quad (2)$$

In Eq. 1, the information from the manifolds generated in all previous iterations has been integrated together in graph \mathcal{G}^t . The ING can thus regulate the graph topologies built on the registered image set \mathbf{I}^t in different iterations and can assure a gentle shift of the global center.

With the global center $I_{c(t)}^t$, the qualified neighbors for

each subject can be determined as follows. First, for the given subject I_i^t at iteration t , we sort all other subjects in an ascending order based on their distances to I_i^t , and a subscript set \mathbf{P}_i^t is built to include the top p_i^t indices. Second, we examine all subjects in \mathbf{P}_i^t and find those that are closer to the current global center $I_{c(t)}^t$ than to I_i^t , *i.e.*, $\mathbf{M}_i^t = \{j | d(I_j^t, I_{c(t)}^t) \leq d(I_i^t, I_{c(t)}^t), j \in \mathbf{P}_i^t\}$. Thus, all the qualified neighbors of subject I_i^t form a set $\mathbf{J}_i^t = \{I_j^t | j \in \mathbf{M}_i^t\}$ and will guide the warping of I_i^t at iteration t .

2.2. Averaging over dense deformation fields

In this section, a mechanism to warp the current subject I_i^t by all its qualified neighbors is defined. We move the subject I_i^t along an average deformation direction on the manifold according to the selected neighbors. To demonstrate the process in a more general situation, the superscript t and the subscript i (indexing the iteration and subject, respectively) are dropped.

Assuming that I is the current subject to be registered, all qualified neighbors selected in Sec. 2.1 form a set $\mathbf{J} = \{J_1, J_2, \dots, J_m\}$ ($m \geq 1$). Our goal is to move I to a new location I' which should be closer to its destination in the end of registration. It can be achieved by averaging the warping directions from I to each J_s ($s = 1, 2, \dots, m$). For each pair of subject I and J_s , the dense deformation field G_s is estimated, and then, its inversed deformation field G_s^{-1} is calculated. Therefore, the average direction can be calculated based on G_s^{-1} (since they are defined on the same image space of I). To emphasize the effect of those neighbors which are closer to the center subject I , we can go one step further by weighting different G_s^{-1} based on the distance $d(I, J_s)$, *i.e.*,

$$G = \left(\frac{\sum_{s=1}^m \omega(d(I, J_s)) G_s^{-1}}{\sum_{s=1}^m \omega(d(I, J_s))} \right)^{-1}, \quad (3)$$

where $\omega(x) = \frac{1}{\sigma\sqrt{2\pi}} e^{-\frac{x^2}{2\sigma^2}}$ and the std σ is adaptively set to be the median value of $\{d(I, J_s) | s = 1, 2, \dots, m\}$.

For each I_i^t , we apply the above procedure to generate the deformation field G_i^t by Eq. 3, and deform it following $I_i^{t+1} = G_i^t(I_i^t)$ to move closer to the current global center. In the following iteration, the distribution of the dataset in the image space becomes much denser, and this self-organized registration can proceed as described above.

2.3. Hierarchical registration structure

As the registration proceeds, it is possible that several nearby subjects converge spontaneously, thus partitioning the image set into subgroups. In this case, the qualified neighbor selection for one subject will be restricted within the subgroup it belongs to. To break this partition and refine the groupwise registration result, we employ a new

strategy to perform registration across different subgroups.

Given a set of registered images, a clustering method (*e.g.*, Affinity Propagation (AP) [18]) can be adopted to bundle those aligned subjects into subgroups. Then, the representative image of each subgroup, automatically determined by the clustering method, forms a new dataset of a much smaller size. The same processing in Sec. 2.1 and 2.2 can be applied on the new dataset (at a higher level), to further register subgroups of images together.

Note that after performing the bundling process, all images in one subgroup will have the same neighbors from the representative image set which are selected by its own representative image. The detail of the hierarchical registration framework is described as follows. All the subjects in the population are first placed on the bottom level and the self-organized registration is performed. Then we apply AP clustering to detect whether the registered images have fallen into a stable partition. If the clustering results on \mathbf{I}^t and \mathbf{I}^{t+1} are not exactly the same, both the self-organized registration and the clustering on the population are repeated on \mathbf{I}^{t+1} . If at some iteration t^* , the clustering results on datasets \mathbf{I}^{t^*} and \mathbf{I}^{t^*+1} do not change, the proposed groupwise registration framework will go to the next level and initiate a new image set containing all representative images. The same procedures are repeated on this new image set, and the registration will terminate once the representative images are clustered into a single group, or the maximal number of levels is reached. In the upmost level, all subjects are registered very close to each other, and therefore we can take the average image as the final atlas. Note that, since the whole population has already been well aligned, the average image is no longer fuzzy, but of clear anatomical structures and sharp boundaries.

It is worth noting that the way of employing the clustering method in our framework is quite different from that in [4]. Clustering is intrinsic to our framework where spontaneous partition happens during registration, rather than a pre-processing step to guide the registration. Any clustering techniques could be adopted in the framework, *e.g.* K-means [19]. But unlike K-means, we do not have to specify the cluster number in AP and the representative image of each cluster is given automatically by AP. The local means and the global mean are both updated dynamically during the registration, which also differentiates ABSORB from other pure clustering methods. Another difference is on how to provide an image for registration in the higher level. In [4], the mean image of each cluster contributes to the registration at the higher level, which suffers from the same problem of using fuzzy mean image as a template as in [7]. On the contrary, in ABSORB, the representative image of each cluster is sent to the higher level, which is a warped individual image with all key anatomical structures, and the groupwise registration accuracy at a higher level can be guaranteed.

3. Experiments

In this section, extensive experiments on both synthetic and real datasets are performed to show the performance of ABSORB. For comparison, the results from the group mean method [7] and the tree-based registration method [13], are also provided. In all experiments, we set the maximum levels of the built hierarchical structure as 4, and the weight factor $\alpha = 0.5$ in (1).

3.1. Synthetic dataset

A synthetic dataset with 61 images simulating the sulci and gyri around the cortical region in MR brain images is shown in Fig. 2(a). From the central image with a single wide gyrus, three different types of images are generated. Each type has 20 images with four of them shown in each branch of the Y-shaped structure in Fig. 2(a).

After performing the groupwise registration with all three methods, the registered images are placed in the same location of the Y-shape structure in Fig. 2(b-d). The group mean method cannot register the images with two or three gyri together since the bottom part of the sulcus is lagging behind the motion of its neighboring anatomies during the registration and thus a deep fissure is formed with a similar depth at the corresponding position of each sulcus. This is resulted mainly because the group mean image is initially very blurry, and it is very difficult for those sulci parts to warp towards the right direction consistently. In Fig. 2(c) and (d), the results of tree-based method and ABSORB are shown together with the final built atlas, respectively. The results of the tree-based method are visually similar to those of ABSORB because the root node is selected to be very close to the geometrical mean. We can see that all the images with different number of sulci and different depth of each sulcus have been well registered onto the final atlas.

We illustrate the registration process of ABSORB on the synthetic dataset in Fig. 3(a-d). The original dataset (red points) is projected onto a 2D space by the Principal Component Analysis (PCA), and the updated image set in all later iterations is projected onto the same 2D space to visualize the converging process. The population is converging in Fig. 3(a-c), with the moving direction of each subject determined by both its qualified neighbors and the (tentatively estimated) global center. After 16 iterations, it reaches a stable distribution, and all representative images form a new dataset and move up to the next level (Fig. 3(c)). On the second level, the same procedure is applied to a much smaller population. Finally, the whole registration process arrives at the top level where all images are registered well and clustered into a single group (Fig. 3(d)).

For comparison, the registration results by the group mean method and the tree-based method on the same 2D projection space are shown in Fig. 3(e) and (f). It is shown

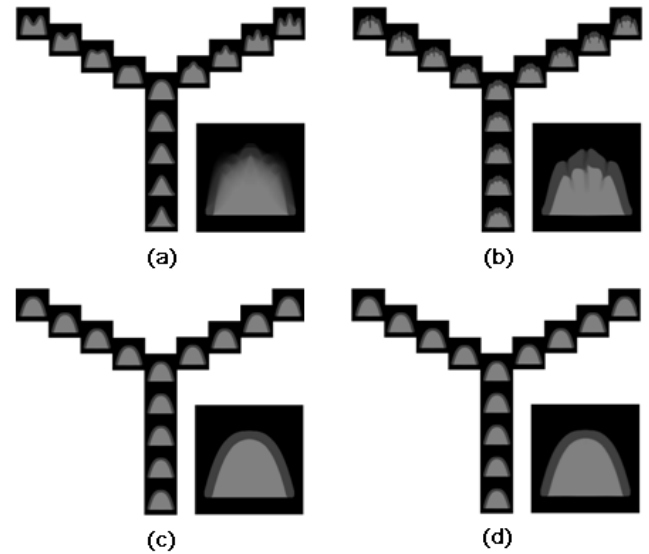


Figure 2: The experimental results on the synthetic dataset: (a) the original images and the blurry mean image, the registration results by (b) the group mean method, (c) the tree-based method (c), and (d) ABSORB. The final atlas built by each method is also shown to the bottom right of each plot accordingly.

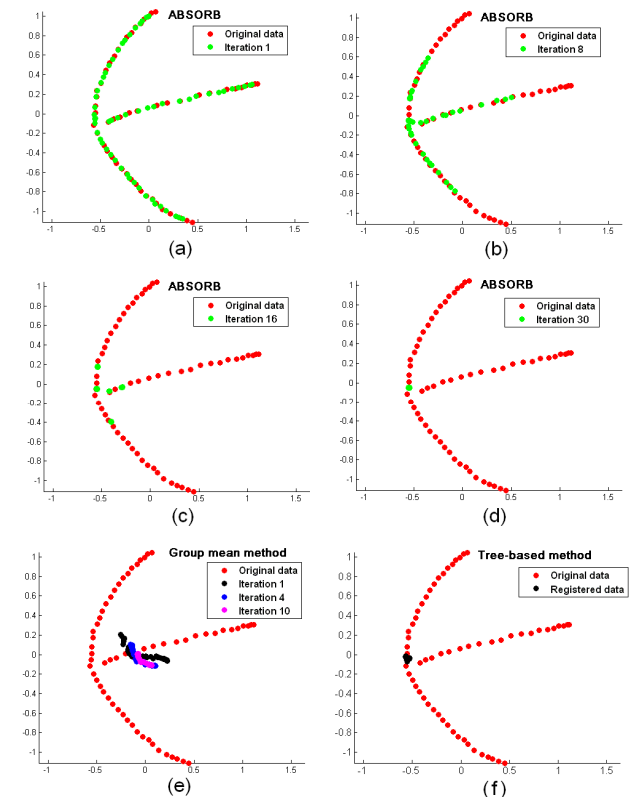


Figure 3: The illustration of the registration process of ABSORB on the synthetic dataset (a-c). The registration results of ABSORB (d), the group mean method (e) and the tree-based method (d) are also displayed, respectively.

that the registration results of ABSORB are much more compact than that of the group mean method. In Fig. 3(e), we can see that, after the first iterative registration by the group mean method, the warped dataset travels away from the manifold (*i.e.*, the data structure represented by three branches) because of the use of initially very fuzzy mean image as shown in Fig. 3(a). In Fig. 3(f), the registration result of tree-based method is also shown, which is not as dense as that of ABSORB.

3.2. Real dataset

A brain MR image dataset with 18 subjects is used to further evaluate the performance of ABSORB on real images with large anatomical variations. First, we visually compare the atlases generated by three different methods in Fig. 4. It can be seen that the atlas image from ABSORB (Fig. 4(c)) is slightly sharper than that of the group mean method (Fig. 4(b)), although they are quite similar to each other. The atlas from the tree-based method (Fig. 4(e)) is biased to the selected root image (Fig. 4(d)), although it is sharper. From the result of the tree-based method on both synthetic and real datasets, we can see that, if the selected root image cannot represent the dataset, the registration process, as well as the built atlas, will be deviated from the group center.

The improvement of ABSORB can be examined more clearly by measuring the overlap rates on different tissues, *i.e.*, white matter (WM), grey matter (GM), and ventricle (VN), and the average entropy on the registered tissue-segmented images. Here, we use the Jaccard Coefficient to measure the similarity between two regions, which is defined as $J(U, V) = |U \cap V| / |U \cup V|$ for two aligned region U and V , where $|\cdot|$ defines the area of region under consideration. The average overlap rates of different ROIs in the registered image set are provided in Table 1. Our method achieves the best overlap rates on all three different tissues, and the average increase over the other two methods is about 4.0%. The average entropy of our method on the aligned tissue-segmented images is 0.17, which is about 10% better than the group mean method and the tree-based method.

The robustness to the outliers of different registration methods is also compared. The registration results of three methods are shown in Fig. 5 by projecting all the registered subjects onto the same 2D space. It can be observed that the final registered images of ABSORB and the tree-based method are more concentrated around the geodesic mean than those of the group mean method. In other words, the group mean method is easily to be distracted by the outliers, *e.g.*, the left-most and the bottom points in Fig. 5(a). It is worth noting that the registration results of ABSORB and the tree-based method are also more densely distributed in the space than those of the group mean method.

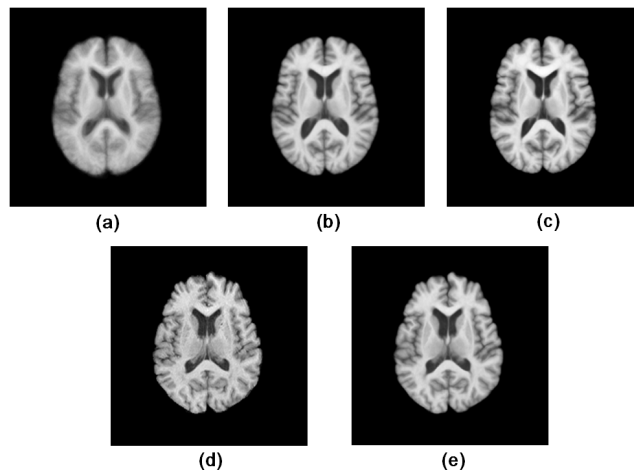


Figure 4: The mean image for the original dataset (a), the atlas image constructed by the group mean method (b), and the proposed ABSORB method (c) are shown in the top. For the tree-based method, its selected root image and the corresponding atlas are shown in (d) and (e), respectively.

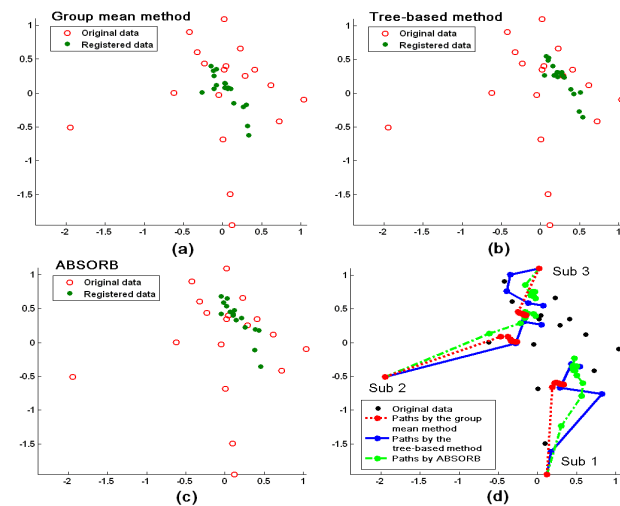


Figure 5: The registration results of the group mean method (a), the tree-based method (b), and ABSORB (c) on 18 elderly brain images are projected on the same 2D subspace. The registration paths produced by three different methods are delineated in (d).

Table 1. The average overlap rates and average entropy on the registered segmentation images.

	Overlap rate (%)			Entropy
	GM	WM	VN	
Original data	35.5%	45.4%	48.6%	0.33
Group mean	49.0%	68.0%	72.6%	0.19
Tree-based	51.7%	61.9%	74.6%	0.19
ABSORB	54.0%	71.0%	76.6%	0.17

The registration paths are also examined in Fig. 5(d) to compare the smoothness of paths generated by different methods. We select three different subjects (as labeled in

Fig. 5(d)), and the registration path for each of them is delineated by connecting all segments from its original position to the final position. It can be seen that the path generated from our method is always much smoother and more direct to the final location than that of the tree-based method, which is more twisted and devious. The main reason is that each deformation segment along the path of our method is the result of averaging several different moving directions, and also that different segments on the same path share a similar direction to the global center. However, in tree-based method, the path is pre-determined by a tree and a fixed root before image registration starting, without considering the dynamic change of overall distribution of the dataset after iterations. Also, the moving directions of different segments on the same path are independently estimated in the tree-based method, thus potentially resulting in a more zigzag path and affecting the registration results. The paths generated by the group mean method become nearly unchanged after the first round of registration, which indicates that the group mean method could be easily trapped by the local minima.

To demonstrate the performance of ABSORB on a large dataset, we apply all three methods on a dataset with 161 real brain MR images. The measurements on overlap rates and average entropy are listed in Table 2. ABSORB still ranks top on all measurements.

Table 2. The average overlap rates and average entropy on the image dataset with 161 subjects for different methods.

	Overlap rate (%)			Entropy
	GM	WM	VN	
Original data	36.8%	45.9%	48.3%	0.37
Group mean	49.9%	68.1%	71.8%	0.21
Tree-based	51.2%	54.4%	74.6%	0.25
ABSORB	55.0%	71.1%	74.7%	0.19

4. Conclusion

A new groupwise registration framework, called Atlas Building by Self-Organized Registration and Bundling, or ABSORB, has been presented. Two novel strategies, self-organized registration and image bundling are employed to perform the groupwise registration hierarchically by automatically building a pyramid of images during the registration procedure. Extensive experiments have been conducted to show that ABSORB can perform the registration more accurately and consistently, compared to other two popular groupwise registration methods. In the future, we will apply ABSORB to clinical dataset and test its performance in detecting brain abnormalities.

Acknowledgement

This work was supported in part by NIH grants EB006733, EB008760, EB008374, MH088520 and EB009634.

References

- [1] W.R. Crum, T. Hartkens, and D.L.G. Hill. Non-rigid image registration: theory and practice. *British Journal of Radiology*, 77: S140-153, 2004.
- [2] D. Shen and C. Davatzikos. HAMMER: hierarchical attribute matching mechanism for elastic registration. *IEEE Trans. on Medical Imaging*, 21: 1421-1439, 2002.
- [3] T. Vercauteren, X. Pennec, A. Perchant, and N. Ayache. Diffeomorphic demons: efficient non-parametric image registration. *NeuroImage*, 45: S61-72, 2009.
- [4] Q. Wang, L. Chen, P.-T. Yap and D. Shen. Groupwise registration based on hierarchical image clustering and atlas synthesis. *Human Brain Mapping*, accepted.
- [5] E.G. Learned-Miller. Data driven image models through continuous joint alignment. *IEEE Trans. PAMI*, 28: 236-250, 2006.
- [6] S.K. Balci, P. Golland, and W. Wells. Non-rigid groupwise registration using B-spline deformation model. *Proc. Open Source and Open Data for MICCAI*: 105-121, 2007.
- [7] S. Joshi, B. Davis, M. Jomier, and G. Gerig. Unbiased diffeomorphic atlas construction for computational anatomy. *NeuroImage*, 23: S151-160, 2004.
- [8] U. Ziyang, M. Sabuncu, W. Grimson, and C.-F. Westin. Consistency clustering: a robust algorithm for group-wise registration, segmentation and automatic atlas construction in diffusion MRI. *International Journal of Computer Vision*, 85: 279-290, 2009.
- [9] D. Blezek and J. Miller. Atlas stratification. *Medical Image Analysis*, 11: 1361-8415, 2007.
- [10] M.R. Sabuncu, S.K. Balci, M.E. Shenton, and P. Golland. Image-driven population analysis through mixture modelling. *IEEE Trans. on Medical Imaging*, 28: 1473-1487, 2009.
- [11] G. Wu, P.-T. Yap, Q. Wang, and D. Shen. Groupwise registration from exemplar to group mean: extending HAMMER to groupwise registration. *Proc. ISBI*, 2010.
- [12] Q. Wang, P.-T. Yap, G. Wu, and D. Shen. Attribute vector guided groupwise registration. *NeuroImage*, accepted.
- [13] J. Hamm, C. Davatzikos, and R. Verma. Efficient large deformation registration via geodesics on a learned manifold of images. *Proc. MICCAI*, 2009.
- [14] B. C. Munsell, A. Temlyakov, and S. Wang. Fast multiple shape correspondence by pre-organizing shape instances. *Proc. IEEE Conf. on CVPR*: 840-847, 2009.
- [15] S. Tang, Y. Fan, and D. Shen. RABBIT: rapid alignment of brains by building intermediate templates. *NeuroImage*, 47: 1277-1287, 2009.
- [16] M.-J. Kim, M.-H. Kim, and D. Shen. Learning-based deformation estimation for fast non-rigid registration. *Proc. Workshops of IEEE Conf. on CVPR*: 1-6, 2008.
- [17] J.B. Tenenbaum, V.d. Silva, and J.C. Langford. A global geometric framework for nonlinear dimensionality reduction. *Science*, 290: 2319-2323, 2000.
- [18] B.J. Frey and D. Dueck. Clustering by passing messages between data points. *Science*, 315: 972-976, 2007.
- [19] J.A. Hartigan. *Clustering algorithms*. Wiley, 1975.